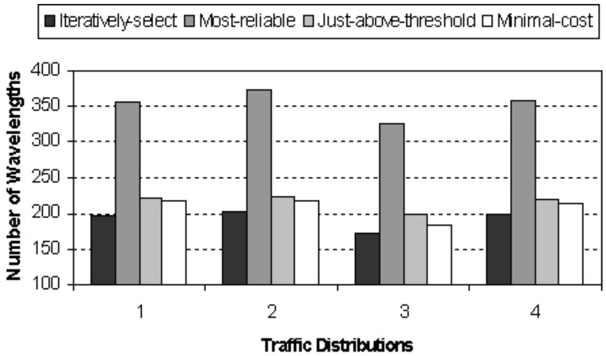

Figure 2: Number of wavelength channels used by heuristic algorithms (without sharing) with different traffic distributions.

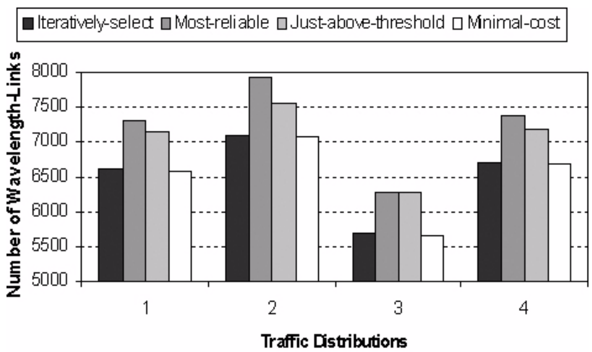

Figure 3: Number of wavelength-links used by heuristic algorithms (without sharing) with different traffic distributions.

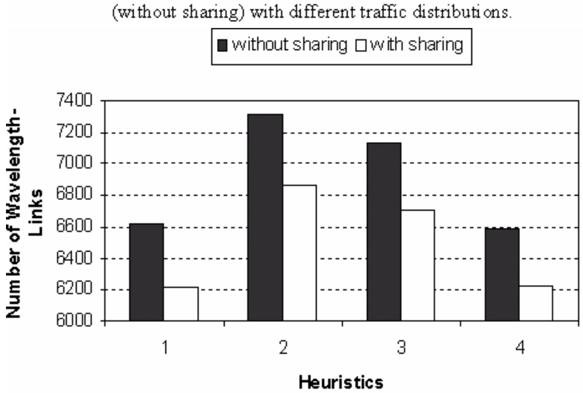

Figure 4: Number of wavelength-links used by heuristics (Iteratively-select, Most-reliable, Just-above-threshold, Minimal-cost, illustrated as heuristics 1 through 4, respectively) with and without resource sharing.

length-channels and around 17% less *W-Links* compared to Scheme II, and provides 99.9% *ASR*. Table 1 also shows performance of heuristics without sharing. All heuristics can provide 100% *ASR* because the route for request *t* is selected from S_t, in which all routes can satisfy availability requirement of *t*. Note that Iteratively-select uses least amount of resources in both *W* and *W-Links* compared to other heuristics and its performance is comparable to that of Scheme III. This is because, in Iteratively-select, either *W* or *W-Links* will be reduced whenever replacing a request's current route by a new one.

Figures 2 and 3 show results of heuristics without sharing for four different traffic distributions - Class I: Class II: Class III: Class IV: Class V = 2:2:2:2:2, 1:1:2:2:4, 4:2:2:1:1, and 1:2:4:2:1 (distributions 1 through 4, respectively). In both figures, observe that Iteratively-select consistently demonstrates better performance than other heuristics; and performance of Most-reliable is worst over all distributions since highly-reliable route is chosen while sacrificing resources. Notice that, in the third distribution, there are more requests with low availability requirement than those in other distributions. In this case, more requests can be provisioned by using a single route; consequently, the third traffic distribution utilizes less resource compared to other distributions (see Figs. 2 and 3).

Figure 4 compares performance of heuristics with and without sharing for traffic distribution 1. Observe that resource-sharing further reduces wavelength-links used in all heuristics (number of wavelengths used is also reduced although not shown here). We find that around 45% requests are unprotected, 30% are dedicated protected, and 25% are shared protected in all heuristics. This percentage varies when traffic distribution changes. Note that resource sharing is achieved without scarifying service reliability.

To conclude, our results indicate that our proposed provisioning framework can help network operators to differentiate network services, improve service reliabilities, and optimize resource efficiency.

References

[1] M. Clouqueur and W. D. Grover, “Availability analysis of span-restorable mesh networks,” *IEEE J. on Selected Areas in Communications*, Vol. 20, No. 4, pp. 810-821, May 2002.

[2] K. C. Chu, M. Mezhoudi, and Y. Hu, “Comprehensive end-to-end reliability assessment of optical network transports,” *Proc., OFC’2002*, pp. 228-230, March 2002.

[3] J. Zhang, K. Zhu, H. Zang, and B. Mukherjee, “A new provisioning framework to provide availability-guaranteed service in WDM mesh networks,” Technical Report No. CSE-2002-30, CS Dept., UC Davis, Sept. 2002.

FA7 **9:45 AM**

Survivable Traffic Grooming in WDM Mesh Networks

C. Ou, K. Zhu, B. Mukherjee, *University of California, Davis, Davis, CA;* H. Zang, *Sprint Advanced Technology Labs, Burlingame, CA;* L. Sahasrabuddhe, *SBC, Inc, San Ramon, CA, Email: ouc@cs.ucdavis.edu*.

We investigate the problem of provisioning shared-mesh-protected sub-wavelength connections in wavelength-convertible optical WDM networks. We propose protection-at-lightpath (PAL) level and protection-at-connection (PAC) level. We found PAL outperforms PAC in such network settings.

1. Introduction

Consider a wavelength-convertible WDM network consisting of optical crossconnects (OXCs) interconnected by point-to-point WDM transmission systems in an arbitrary mesh topology. OXCs can switch traffic at (1) wavelength granularity and (2) at sub-wavelength granularity by dropping a set of wavelengths to the grooming fabric through grooming ports [1]. The number of grooming ports (add and drop) determines the grooming capacity of an OXC.

While the transmission rate of a wavelength is high (typically OC-192 today), the bandwidth requirement of a connection can vary from the full wavelength capacity down to OC-1 or lower. To efficiently utilize network resources, low-speed connections can be groomed onto direct optical transmission channels, or lightpaths. Meanwhile, the failure of a network element can cause the failure of several lightpaths, thereby leading to large data and revenue loss. Fault-management schemes such as protection are essential to survive such failures.

Most previous research on connection provisioning treated *grooming* [2] and *protection* [3] separately. To efficiently provision a survivable sub-wavelength connection, however, grooming and protection need to be considered simultaneously. For dynamically establishing shared-path-protected low-speed connections, reference [4] presented two schemes: mixed working-backup grooming policy and segregated working-backup grooming policy. With both schemes employing fixed-alternate routing, the work focused on the effect of different wavelength-assignment algorithms.

We propose protection-at-lightpath (PAL) level and protection-at-connection (PAC) level for dynamically provisioning shared-mesh-protected sub-wavelength connections against single-fiber failures. Our study differs from previous work [4] in that we focus on the important problem of route computation and the impact of backup sharing.

2. Protection-at-Lightpath (PAL) Level vs. Protection-at-Connection (PAC) Level

Under PAL, the route of a connection is a sequence of *protected lightpaths*. A protected lightpath has a primary path, which carries traffic during normal operation, and a fiber-disjoint backup path, which carries traffic only when the primary path fails. Thus, protection occurs at lightpath level in PAL. Under PAC, a connection has fiber-disjoint primary and backup paths, each of which is a sequence of *unprotected lightpaths*. An unprotected lightpath can use a portion of its bandwidth to carry sub-wavelength connections and set aside part of its bandwidth as backup resources for other connections. Thus, protection occurs at connection level in PAL. In both cases, a connection only consumes the amount of bandwidth it requires.

We illustrate PAL and PAC via an example. For the network in Fig. 1(a), each fiber has two wavelengths of capacity OC-192 each; every node has three grooming ports. Let <*s, d, B*> represent a connection from node *s* to node *d* requiring bandwidth *B*.

2.1 PAL

Upon the arrival of connection c_1, <4, 1, OC-48>, one way of provisioning c_1 under PAL is shown in Fig. 1(b). A protected lightpath l_1, with primary resources *set up* along path <4, 1> and backup resources *reserved* along path <4, 0, 1>, consumes an add port at node 4 and a drop port at node 1. The free capacity of l_1 is OC-144. Note that wavelengths for l_1's backup path have been reserved, but they are not set up as a lightpath. Thus, the backup path does not consume grooming ports when it does not carry traffic. When the primary path fails and the backup path needs to carry traffic, it can reuse the grooming ports previously used by the primary path.

Suppose c_1 remains in the network when connection c_2, <4, 2, OC-48>, arrives. One way of provisioning c_2 under PAL is shown in Fig. 1(c). A protected lightpaths l_2 is set up from node 4 to node 2 with free capacity OC-144. Because l_2's primary path <4, 3, 2> is fiber-disjoint to l_1's primary path <4, 1>, l_2's backup path <4, 0, 1, 2> can share the wavelengths on links <4, 0> and <0, 1> with l_1's backup path. l_2 consumes an add port at node 4 and a drop port at node 2.

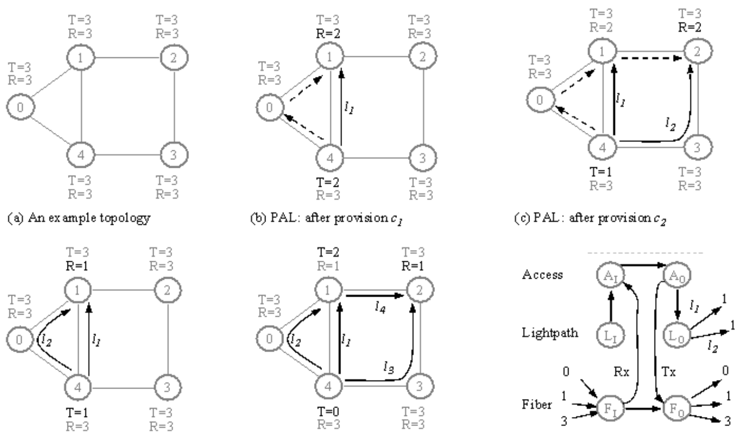

(a) An example topology (b) PAL: after provision c_1 (c) PAL: after provision c_2

(d) PAC: after provision c_1 (e) PAC: after provision c_2 (f) Representation of node 4 in Fig. 1(d)

Figure 1. Provision connections c_1, (<4, 1, OC-48>) and c_2, (<4, 2, OC-48>) under PAL and PAC (T and R represent the number of add and drop ports, respectively.)

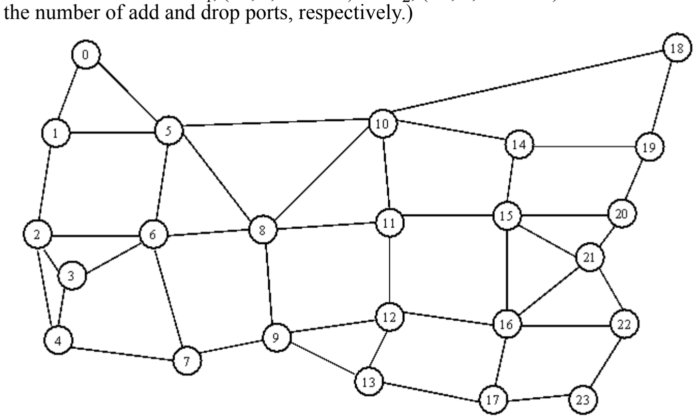

Fig. 2. A 24-node 86-fiber network used in our simulation.

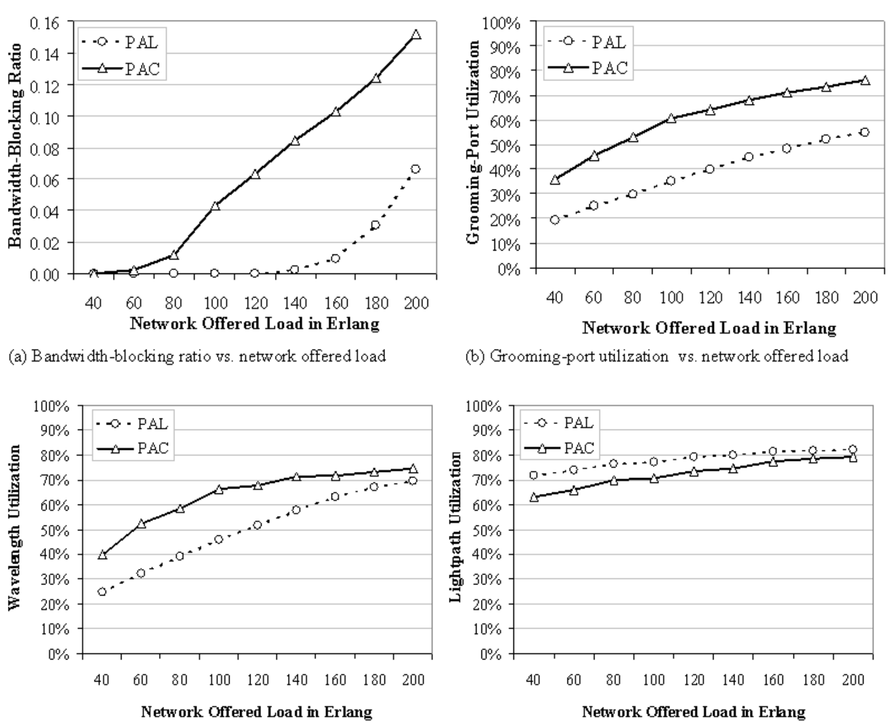

(a) Bandwidth-blocking ratio vs. network offered load (b) Grooming-port utilization vs. network offered load

(a) Wavelength-utilization vs. network offered load (b) Lightpath utilization vs. network offered load

Figure 3. Illustrative numerical results. (Load is defined as connection-arrival rate times average holding time times connections' average bandwidth in the unit of OC-192.)

2.2 PAC

Upon the arrival of c_1, one way of provisioning c_1 under PAC is shown in Fig. 1(d). Two unprotected lightpaths l_1 and l_2 are set up. c_1's primary path traverses l_1 and backup path traverses l_2. Both lightpaths l_1 and l_2 consume an add/drop port. The free capacity of both lightpaths is OC-144. The backup capacity reserved on l_1 is zero. The backup capacity reserved on l_2 is OC-48, and it is used to protect c_1's primary path.

Suppose c_1 remains in the network when c_2 arrives. One way of provisioning c_2 under PAC is shown in Fig. 1(e). Two more unprotected lightpaths l_3 and l_4 are set up. The primary path of c_2 traverses l_3. The backup path of c_2 traverses l_2 and l_4. Both lightpaths l_3 and l_4 consume an add/drop port. The remaining capacity on all the four lightpaths is OC-144. The backup capacity on l_1 and l_3 is zero. The backup capacity reserved on l_2 is OC-48 (c_1 and c_2 share the backup capacity) and it is used to protect the primary paths of c_1 and c_2. The backup capacity reserved on l_4 is OC-48 and it is used to protect c_2's primary path. Alternatively, c_2's backup path could have traversed l_1 and l_4 instead of l_2 and l_4. In that case, OC-48 capacity of l_1 is used by c_1's primary path and another OC-48 capacity of l_1 is reserved by c_2's backup path.

2.3 PAL vs. PAC

The fundamental difference between PAL and PAC is that PAL provides end-to-end protection with respect to lightpath while PAC provides end-to-end protection with respect to connection. When a failure occurs, under PAL, the end nodes of the affected protected lightpaths switch to their backup paths; the affected connections are oblivious to the protection-switching process. Under PAC, the end nodes of the affected connections (which might outnumber the affected lightpaths significantly) switch to their backup paths. Generally, PAL performs at an aggregate level (lightpath) and PAC works on a per-flow basis (connection).

3. Connection-Provisioning Heuristics

To provision a connection request, our heuristics first represent as an auxiliary graph the current network state (including existing lightpaths, available wavelengths, and free grooming ports); then they compute routes based on the graph and appropriate backup-sharing measurements. To conserve space, route-computation details are not presented here.

To represent the network state, we adopt the work in [5], which models a network as an auxiliary graph and represents various resources as edges in the graph by expanding a network node into different vertices. Figure 1(f) shows the expanded node 4 in Fig. 1(d): grooming ports are represented as edges <F_I, A_I> and <A_O, F_O>; existing lightpaths starting at node 4 are mapped to edges sourced at vertex L_O; and incoming (outgoing) fibers are denoted as edges ending at F_I (starting at F_O).

To measure backup-sharing potential in PAL, we associate to a fiber a conflict set, which defines the number of wavelengths to be used to protect against each possible single-fiber failure. The number of wavelengths to be reserved on a fiber is the maximum of its conflict set. In PAC, we associate to a lightpath a conflict set, which defines the amount of bandwidth to be used to protect against each possible single-fiber failure. The amount of bandwidth to be reserved on a lightpath is the maximum of its conflict set.

4. Illustrative Results and Analysis

We simulated a dynamic network environment with the following assumptions: connection-arrival process is Poisson; connection-holding time follows a negative exponential distribution; the number of connections follows the distribution OC-1: OC-3: OC-12: OC-48: OC-192 = 300: 20: 6: 4: 1 (these ratios, provided by our colleagues in the carrier world, are close to reality); connections are uniformly distributed among all node pairs; the topology with 16 wavelengths per fiber is shown in Fig. 2; wavelength capacity is OC-192; the number of grooming ports at a node is set as the number of wavelengths times its nodal degree times a scalar Δ ($0 \le \Delta \le 1$). We report results with Δ=0.7 here (different values of Δ led to the same conclusion).

Figure 3(a) compares the bandwidth-blocking ratio (BBR) of PAL and PAC. BBR is defined as the amount of bandwidth blocked over the amount of bandwidth offered. We observe that PAL has much lower BBR.

The main reason for this is that, in PAL, the backup path of a protected lightpath is *reserved, but not set up*. This also results in lower grooming-port utilization in PAL (Fig. 3(b)) because the backup paths of protected lightpaths do not consume grooming ports.

The second reason lies in the backup-sharing measurement. In PAC, the backup path of a connection has fixed route and fixed wavelength. In PAL, however, the backup path of a protected lightpath only has fixed route: the reserved wavelengths on a fiber act like a "pool" for all the failure scenarios. Further results that PAL has lower wavelength utilization (Fig. 3(c)) and higher lightpath utilization (Fig. 3(d)) verify the advantage of pool reservation [6].

Third, in PAL, two protected lightpaths traversed by a connection can still share backup resources as long as their primary paths are fiber-disjoint. PAC, however, does not have this freedom.

5. Conclusion

Under today's connection distribution where lower-bandwidth connections outnumber higher-bandwidth connections, PAL outperforms PAC in wavelength-convertible networks with shared-mesh protection. For wavelength-continuous networks, this conclusion is found to hold for typical network settings, although the difference in performance between PAL and PAC is reduced.

An interesting variation of PAC is to reserve wavelengths (not to set up as lightpaths) for backup paths. The results of this variation (not included here due to space limitation) largely depend on Δ.

References

[1] K. Zhu and B. Mukherjee, "On-line approaches for provisioning connections of different bandwidth granularities in WDM mesh networks," *OFC02*, ThW5.

[2] J. M. Simmons et al, "Quantifying the benefit of wavelength add-drop in WDM rings with distance-independent and dependent traffic," *IEEE/OSA JLT*, Jan. 1999.

[3] G. Ellinas et al, "Routing and restoration architectures in mesh optical networks," *SPIE ONM*, 2002.

[4] S. Thiagarajan and A. Somani, "Traffic grooming for survivable WDM mesh networks," *OptiComm*, 2001.

[5] H. Zhu et al, "A novel, generic graph model for traffic grooming in heterogeneous WDM mesh networks," *IEEE/ACM Trans. Networking*, 2003.

[6] S. Datta et al, "Efficient channel reservation for backup paths in optical mesh networks", *IEEE GLOBECOM*, 2001.

FB 8:00 AM - 10:00 AM

B308-B309

Novel Materials

Martin Fermann, *IMRA America, USA, Presider*

FB1 8:00 AM

Gain Characteristics of Thulium-Doped Tellurite Fiber Amplifiers by Dual-Wavelength (800nm + 1064 nm) Pumping

A. Cucinotta, F. Poli, S. Selleri, *University of Parma, Parma, Italy, Email: stefano.selleri@unipr.it.*

We demonstrate that simultaneously pumping a thulium-doped tellurite fiber amplifier with 800nm and 1064nm significantly increases the achievable gain. A gain of 26dB and noise figure less than 4dB were obtained with a 1.5m doped fiber length.

Introduction

The growing demand for higher transmission capacity requires optical fiber amplifiers that can fully exploit the low loss region of optical fibers (1450-1650 nm). Erbium-doped fiber amplifiers have been successfully employed in the C- and L-bands in silicate as well as tellurite-based fibers [1].

Thulium-doped amplifiers are very promising candidate to achieve amplification in the shorter wavelength band (1480-1530nm). Thulium-doped fluoride fiber amplifiers have been demonstrated to operate both in the S+-band (1450-1480 nm) [2] as well as in the S-band by developing gain-shifted thulium-doped fiber amplifiers [3], [4]. In particular many efforts have been spent in order to study the pumping scheme impact on the amplifier performances [3], [5],[6].

New challenges are opened by the possibility of using Tm^{3+}-doped tellurite fibers instead of fluoride ones [7]. Infact one possible solution to fabricate broadband amplifiers is the selection of glass hosts with high refractive-index, because the stimulated emission cross section σ_e increases with the refractive-index value according to $\sigma_e \approx (n^2+2)^2 / n$. Therefore, it becomes possible to obtain optical gain over a broader wavelength range than with hosts having lower refractive-index. From this point of view, tellurite glasses, the main component of which is TeO_2, have the advantage of enhancing the cross-sections because their refractive index is larger than 2. The optical properties of Tm^{3+}-doped tellurite glasses have been studied in [8] and [9] where the good properties of tellurite glasses are highlighted.

In this paper the gain characteristics of Thulium-Doped Tellurite Fiber Amplifiers (TDTFAs) are investigated by a dual-pumping scheme (800nm + 1064 nm). Results demonstrate that this scheme significantly increases the achievable gain. 100mW pump power at 800nm yielded a gain enhancement of 11 dB. A gain of 26dB and noise figure less that 4dB were obtained with only 1.5 m doped fiber length. The use of tellurite fibers instead of fluoride ones [10] allows for a 10 times shorter fiber length. Moreover the gain in tellurite extends by at least 20nm to longer wavelengths than that reported in fluoride.

The dual pumping scheme and doped fiber parameters

The energy level diagram of Tm^{3+} in tellurite is reported in Fig.1. The dual pumping scheme at 800 nm and 1064 nm has been considered. As depicted in Fig.1, the 800 nm pump populates directly the $^3H_4$ level. However the transition $^3H_4 \rightarrow {}^3F_4$ is self-terminating, therefore the up-conversion pumping at 1064 nm is added. This implies ground state absorption (GSA) from level $^3H_6$ to $^3H_5$, very fast decay from $^3H_5$ to $^3F_4$ and excited state absorption (ESA) from $^3F_4$ to $^3F_{2-3}$. The $^3F_2$ and $^3F_3$ levels are very close and they can be regarded as one level, for simplicity. Stimulated emission around 1470 nm is due to transition $^3H_4 \rightarrow {}^3F_4$. Spontaneous emission from $^3H_4$ concerns the transitions $^3H_4 \rightarrow {}^3H_6$ (800 nm),

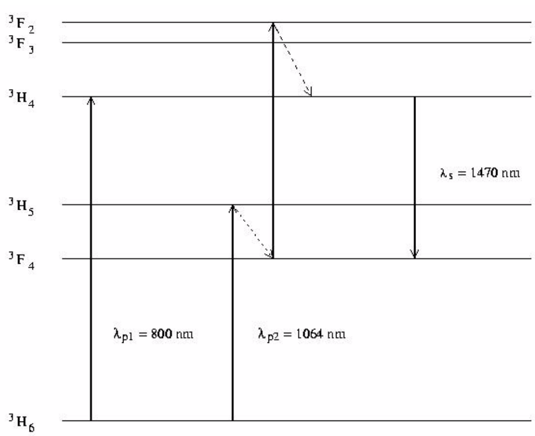

Figure 1. Tm^{3+} energy levels and dual pumping scheme.

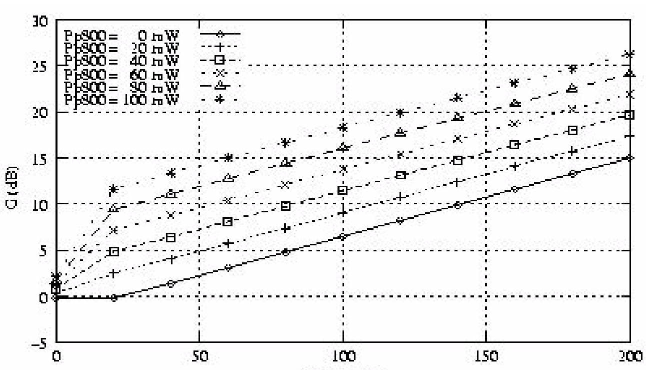

Figure 2. Fiber gain versus pump power at 1064nm for different values of pump power at 800nm.